Electronic Supplementary Material (ESI) for Physical Chemistry Chemical Physics.


Electronic Supplementary Information

# Experimental and theoretical study of multinuclear indium-oxo clusters in CHA zeolite for $CH_4$ activation at room temperature

Zen Maeno*[a], Shunsaku Yasumura[a], Chong Liu[a], Takashi Toyao[a,b], Kenichi Kon[a], Akira Nakayama[a,c], Jun-ya Hasegawa[a], Ken-ichi Shimizu*[a,b]

[a] Institute for Catalysis, Hokkaido University, N-21, W-10, Sapporo 001-0021, Japan

[b] Elements Strategy Initiative for Catalysts and Batteries, Kyoto University, Katsura, Kyoto 615-8520, Japan

[c]JST, PRESTO, 4-1-8 Honcho Kawaguchi, Saitama 332-0012, Japan

*Corresponding authors

Zen Maeno, Ken-ichi Shimizu

E-mail: kshimizu@cat.hokudai.ac.jp, TEL: +81-11-706-9164

## Figures and Tables

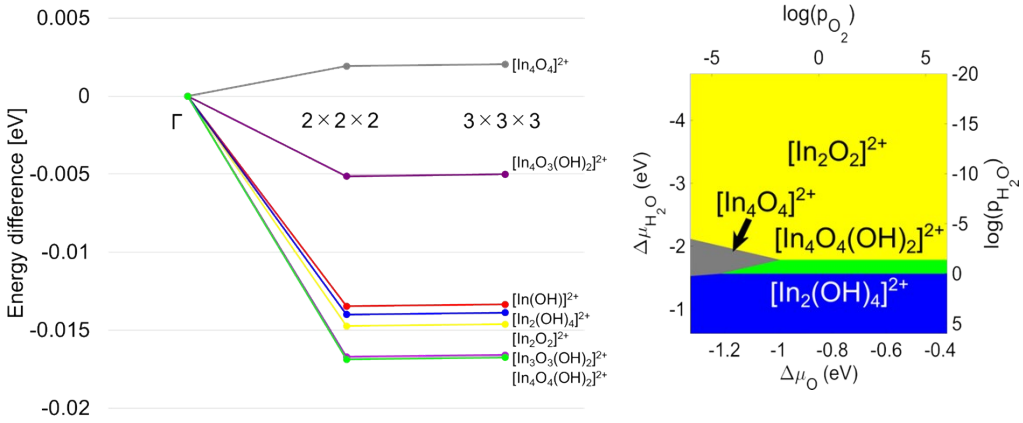


**Figure S1.** Difference of total energy using 2×2×2 and 3×3×3 k point meshes and that using Γ point for each In-oxo ions on 8MR(4NN) (left). The phase diagram for 8MR(4NN) obtained using 2×2×2 k point mesh (right).

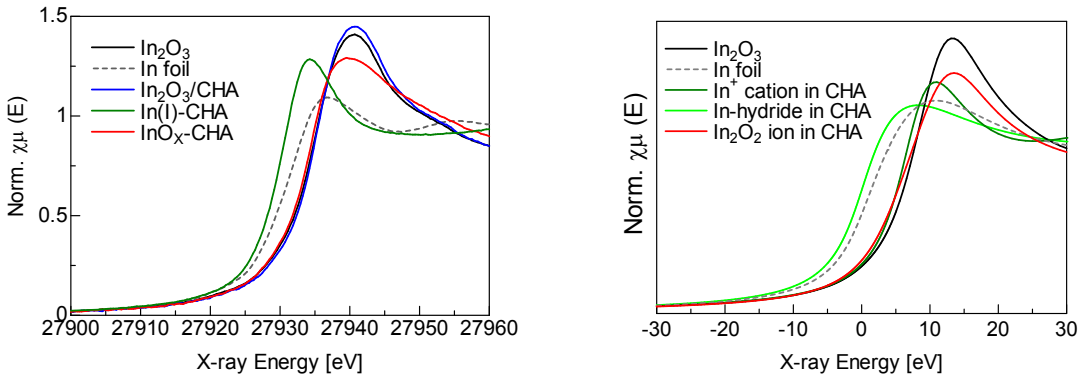


**Figure S2.** Comparison of experimental (left) and simulated (right) XANES spectra of a series of In-CHA and reference In compounds (In foil and $In_2O_3$).

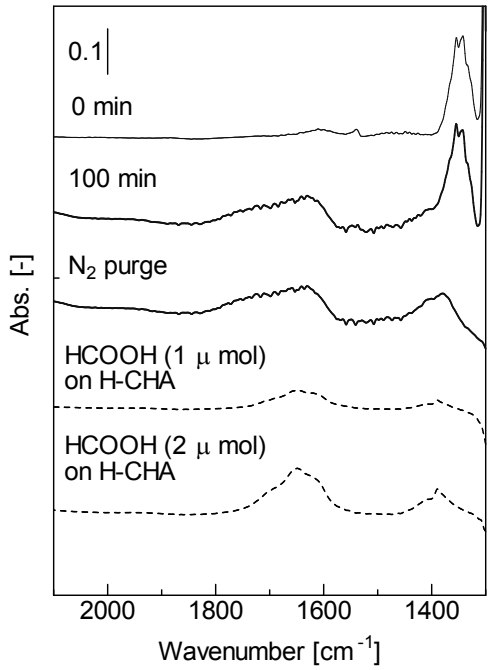


**Figure S3.** FT-IR spectra during reaction of $CH_4$ on $InO_X$-CHA at room temperature and formic acid on H-CHA (as reference).

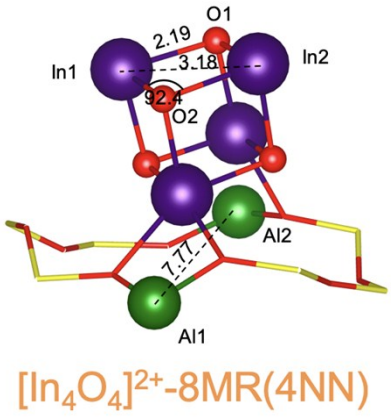


**Figure S4.** Optimized structure of $[In_4O_4]^{2+}$-8MR 4NN

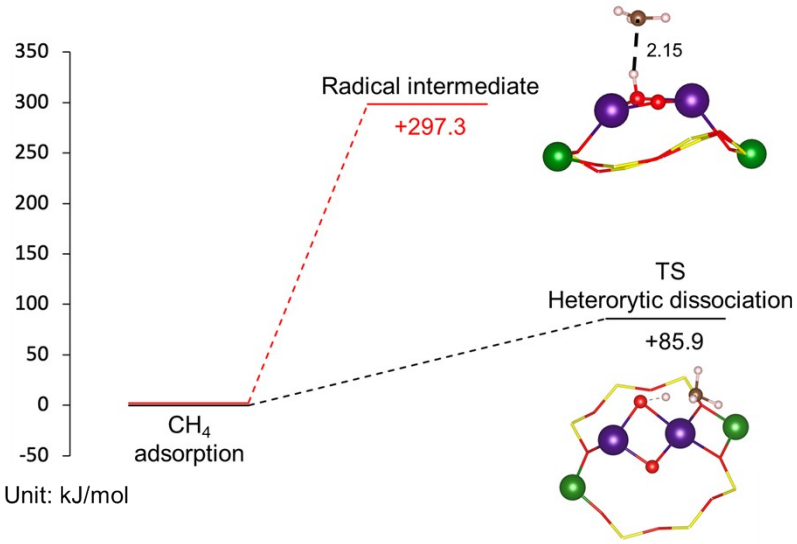


**Figure S5.** Comparison of energy diagrams in C–H cleavage of $CH_4$ on $[In_2O_2]^{2+}$-8MR 4NN through heterolytic path (lower) and homolytic path (upper).

**Table S1**. Specific surface areas and pore volumes of zeolites

| Sample | BET surface area ($m^2\ g^{-1}$) | Pore volume ($mL\ g^{-1}$) |
|---|---|---|
| H-CHA | 833 | 0.402 |
| $In_2O_3$/CHA | 785 | 0.378 |
| $InO_X$-CHA | 710 | 0.344 |

**Table S2**. Total energy (eV) of In-oxo ions on 6MR(3NN), 8MR(3NN), and 8MR(4NN)

| In species | 6MR(3NN) | 8MR(3NN) | 8MR(4NN) |
|---|---|---|---|
| $[In(OH)]^{2+}$ | -873.3 | -871.9 | -871.8 |
| $[In_2O_2]^{2+}$ | -876.5 | -877.0 | -877.2 |
| $[In_2(OH)_4]^{2+}$ | -909.2 | -909.4 | -909.0 |
| $[In_3O_3(OH)_2]^{2+}$ | -897.0 | -898.3 | -898.0 |
| $[In_4O_4]^{2+}$ | -897.4 | -897.9 | -898.1 |
| $[In_4O_3(OH)_2]^{2+}$ | -913.2 | -913.9 | -913.5 |
| $[In_4O_4(OH)_2]^{2+}$ | -919.3 | -920.2 | -920.0 |